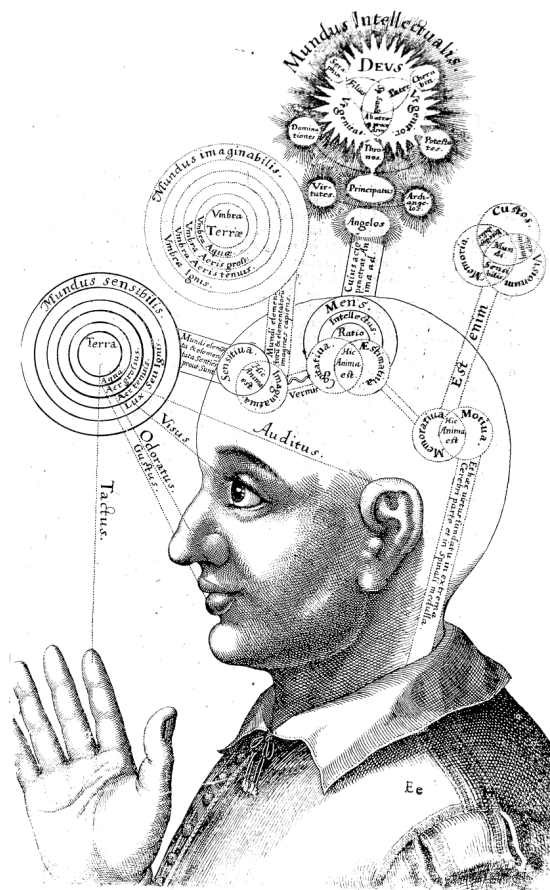


Computational Models of Altered States of Consciousness

Daniel Korsunsky



NEUR 503: Computational Neuroscience
13 April 2022

Introduction

Questions surrounding consciousness and conscious states have fascinated philosophers and cognitive neuroscientists for centuries. Among them, philosopher David Chalmers made the distinction between *the hard problem of consciousness* (why and how we have qualia and phenomenal experiences), and *easy problems* (the task of understanding how the brain gives humans certain abilities, such as making decisions and integrating information). To be sure, the latter problems are meant to be easy only in a relative sense, but with enough funding and brainpower, they are far easier to capture in a computational or mechanistic manner.

As we know from pathological or traumatic insights, what is often illuminating when trying to understand consciousness is looking at instances when it is working differently, such as in the psychedelic or practicing shamanic brain. Thus, our inquiry into the functions and characteristics of consciousness is guided by the following questions, outlined in Carhart-Harris et al. (2014):

How does the normal waking consciousness of healthy adult humans relate to other states of consciousness?

What happens to the brain's functionality in non-ordinary states, such as during the psychedelic or shamanic state?

How does the brain maintain its normal state of waking consciousness?

Recent advances in physics and neuroscience have been converging on a unified theory of how the human brain predicts the environment, forms concepts, and organizes into coherent, hierarchically-structured systems; how normal waking consciousness of healthy adult humans

relates to different states of consciousness; the dynamic relationship between the conscious and unconscious mind; and how this interplay has made *Homo sapiens* the most adaptable species on the planet. Proposed by physicist Karl Friston and neuroscientist Robin Carhart-Harris, the entropic brain hypothesis argues that “the quality of any conscious state depends on the system’s entropy” (Carhart-Harris et al., 2014).

Entropy is the measure of how uncertain we are about the system’s state if we were to sample it at a random time point—in other words, how disordered the system is. For example, increased subjective uncertainty, or surprise, is quantified as higher entropy. According to Friston (2010)’s free energy principle, biological systems, including the brain, maintain order by developing inferences and behaviors that seek to minimize surprise and uncertainty. When compared to the rest of the animal kingdom, the human brain exhibits *greater* entropy, as the human mind possesses a greater repertoire of potential mental states than other animals. By the entropic brain hypothesis, the brain of modern adult humans differs from that of its closest evolutionary and developmental antecedents because of an extended capacity for entropy suppression.

The psychological counterpart of this process is the development of a mature ego and associated metacognitive function: the brain gravitates away from criticality proper¹ toward a state of slight subcriticality, by means of the default mode network (DMN) and other high-level global processing networks (Carhart-Harris et al., 2014). Through these mechanisms of organizing and constraining cognition, the brain can process the environment as precisely as possible. In this state of subcriticality, the brain can exert better control over the resort of the

¹ Criticality is a state occupying a narrow transition window between order and chaos, characterized by a maximum number of metastable or transiently-stable states, maximum sensitivity to perturbation (such as stimuli), and a propensity for cascade-like processes that propagate throughout the system (Carhart-Harris et al., 2014).

natural world, much of which is critical: “If control is the objective, then it makes sense that the brain should be more ordered than that which it wishes to control” (Carhart-Harris et al., 2014).

The findings of Carhart-Harris reveal that psychedelic compounds such as psilocybin, LSD, and ayahuasca inhibit the DMN and other high-level association networks, encouraging a more unconstrained mode of cognition at a more critical state than normal waking consciousness. This promotes connectivity among brain regions that do not typically talk to each other, as seen below in Figure 1.

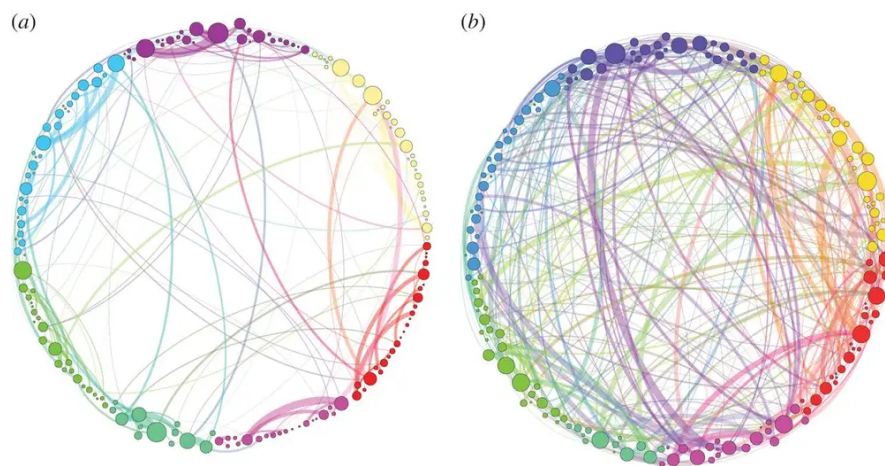


Figure 1. From Petri et al. (2014), the difference in brain connectivity and activity following (a) placebo and (b) psilocybin ingestion. Each node is a brain region.

Because of this heightened connectivity between brain regions that are not otherwise strongly connected, and because of the inhibition of high-level integration networks, the critical brain pays less deference to reality, characterized by less precise sampling of the external world. This reorganization of the brain network explains why LSD study participants and shamanic practitioners reported experiencing higher levels of complex imagery, spiritual experience, insightfulness, changes in the meanings of things, and so on (Huels et al., 2021). Criticality has

also been found to characterize the brain states of experienced meditators and children, and is often described as a state of “magical thinking” (Carhart-Harris et al., 2014; Huels et al., 2021).

As criticality represents a broader repertoire of potential mental states, it correlates with higher levels of entropy and connectivity. In this paper, we will examine different computational methods that seek to distinguish and characterize altered states of consciousness through various measures of entropy, connectivity, and complexity, all of which correlate strongly with each other (Carhart-Harris et al., 2014). Indeed, for our purposes, entropy itself is defined in multiple ways: the complexity of a neural signal, the number of possible connection motifs, or the variance in network synchronization, for example.

We will first examine three methods that evaluate the degree of functional connectivity, complexity, and criticality of time series, such as EEG, MEG, or BOLD signals: these are the (weighted) phase lag index, Lempel-Ziv complexity, and the pair correlation function, respectively. Each of these methods employ broadband as well as single band analysis, to capture the metrics in question based on the level of awareness that corresponds to each band.

We will then examine how to use these brain signals to create connected graphs, and, subsequently, how we can use them to compute and evaluate global and local network characteristics. For each method, we will examine the results and conclusions of relevant computational studies of the effects of psilocybin, LSD, and ayahuasca on the brain, as well as of the brains of shamanic practitioners. While some of the effects of these psychedelics are both different from shamanic trance and from each other, they have all been found to similarly influence the metrics in question. Thus, for our purposes, we will treat them as equivalent. In this essay, the term “altered states of consciousness” will refer exclusively to those states characterizing the psychedelic and practicing shamanic brains.

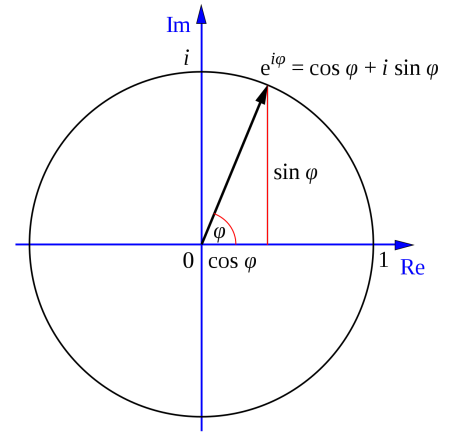
Time Series Analysis

Functional Connectivity

Functional connectivity is defined as the strength to which activity between a pair of brain regions covaries or correlates over time—in other words, the temporal coincidence of spatially distant neurophysiological events (Friston, 1994). Thus, areas are presumed to be coupled or are components of the same network (exhibiting functional connectivity) if their functional behavior is consistently correlated with each other (Eickhoff and Müller, 2015).

Intuitively, functional connectivity is considered a reliable model for characterizing altered states of consciousness because it indicates the degree to which typically less-connected brain regions are talking with one another. A common model for assessing functional connectivity is the phase lag index, or PLI, which measures the consistency of phase locking: the presence of consistent, nonzero phase difference between the signals of two regions suggests that these regions are functionally connected.

By computing the cross-spectrum of two signals, we obtain a vector whose angle with the real axis represents the phase difference between the signals (seen in the image to the right). Phase synchronization, accordingly, can be understood statistically as the stability or consistency of phase difference between two time series over time. The phase angle can be computed as follows:



$$\phi = \arctan\left(\frac{\text{imag}[\tilde{C}(f)]}{\text{real}[\tilde{C}(f)]}\right)$$

where the $C(f)$ is the cross-spectrum. The phase lag index (PLI), proposed by Stam et al. (2007) has the following equation:

$$PLI = \left| n^{-1} \sum_{t=1}^n \text{sgn}(\text{Im} \left[e^{i(\phi^j - \phi^k)_t} \right]) \right|$$

which applies the signum function (1 if $x > 0$, 0 if $x = 0$, and -1 if $x < 0$) to the imaginary component of phase difference at each timepoint k , and then takes the absolute value of the average.

The signum function and imaginary component are perhaps the least obvious element of this approach, and were introduced to solve the problem of *volume conduction*, which occurs when electrodes record electrical signals at a distance from the source². Because volume conduction is instantaneous in time, an observed phase difference of 0 could mean that the two electrodes are picking up the same signal, which is not true phase-locking. This problem can also be characterized by a phase lag of π radians if one of the electrodes sees the other end of the source dipole and thus records a negative voltage (Subramaniam, 2019). Thus, the imaginary component computes the phase difference mod π , and the signum function subsequently discards phase differences of $0 \bmod \pi$. Non-zero ($\bmod \pi$) phase difference must represent true leading or lagging, characterized by a phase difference angle above and below the real axis, respectively.

Since the PLI computes the absolute value of the average signed phase lag, it only cares if the cross spectrum is consistently above or below the real axis (whether one brain region consistently leads or lags behind another). Thus, PLI does not give any info about the direction of interaction (which brain region leads the other). The PLI ranges between 0 and 1, with 0 indicating no coupling and 1 indicating true, lagged interaction. Thus, the PLI reflects the

² This is mainly a problem for EEG-based studies.

proportion of phase difference between signals over time above or below the real axis. For example, comparing the two plots in Figure 2 below, if the cross-spectrum looks like the figure on the left, with half of the vectors projecting on the positive imaginary axis, and half on the negative imaginary axis, the PLI would be 0. If the cross-spectrum looks like the figure on the right (or if all vectors were pointing down), the PLI would be 1.



Figure 2. Two phase coupling distributions from Cohen (2015). The distributions represent a PLI value of 0 and a value of 1, respectively.

As we've seen, PLI sacrifices true synchronization to get rid of artifacts, but some studies have shown that PLI strongly underestimates the connectivity at small time lags and low signal-to-noise ratio (Cohen, 2015). While PLI reduces Type I errors (falsely identifying connections due to volume conduction), it can produce high Type II errors (ignoring true connections). Indeed, measurements of local field potentials showed that these Type II errors may be exceptionally high (Thiagarajan et al., 2010). These shortcomings merit serious attention, but they are not as consequential when applying the PLI to characterizing the psychedelic or practicing shamanic brain: especially because the PLI does not miss true connectivity, it will reliably pick up the *relative increase* in functional connectivity in these altered states of consciousness, which is the primary objective of this computational inquiry. This method is also useful when targeting the statistical connectivity between specific brain regions of interest.

As an extension of the PLI, the weighted PLI (wPLI) was introduced to de-weight phase differences close to $0 \bmod \pi$, such that those phase values would have a smaller impact on the PLI (Vinck et al., 2011). In this metric, the contribution of observed phase differences is weighted by the magnitude of the imaginary component of the cross-spectrum, $\Im[X]$:

$$\text{wPLI} = \frac{|E\{\Im\{X\}\}|}{E\{|\Im\{X\}|\}} = \frac{|E\{|\Im\{X\}|\text{sgn}(\Im\{X\})\}|}{E\{|\Im\{X\}|\}}$$

Vinck et al. (2011) demonstrate that the wPLI has two advantages over the bare PLI: reduced sensitivity to additional, uncorrelated noise sources and increased statistical power to detect changes in phase-synchronization.

In their study on shamanic practitioners (see Figure 3), Huels and colleagues (2021) instructed practitioners to conduct shamanic healing while listening to a drumming recording, during which the practitioners entered an altered state of consciousness to glean information to be used for the physical, psychological, or spiritual healing of a client not present during the study (control participants were just asked to close their eyes during the trial). The researchers found that shamanic practitioners had increased low beta (13-20 Hz) and decreased low alpha (8-10 Hz) wPLI functional connectivity during drumming compared to control participants. This makes intuitive sense, since beta bands correspond to a state of alertness, while alpha waves correspond more to a state of relaxation. These results corroborate expectations that altered states of consciousness are characterized by higher functional connectivity than normal waking consciousness.

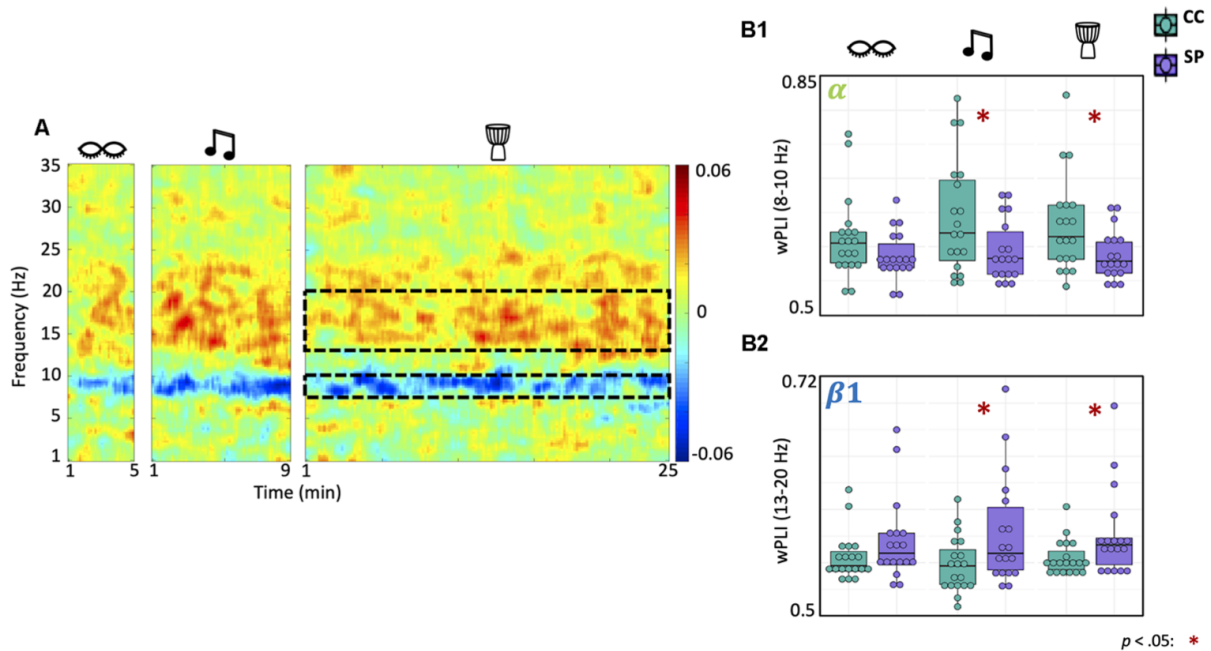


Figure 3. The figures above from Huels et al. (2021) demonstrate that shamanic practitioners (SP) have increased low beta (13-20 Hz) and decreased low alpha (8-10 Hz) connectivity during drumming compared to control participants (CC). **(A)** The heatmap demonstrates differences in functional connectivity by band frequency, measured by the wPLI, between shamanic practitioners and the control group: warmer colors represent greater connectivity in SP while cooler colors indicate greater connectivity in CC. **(B1,B2)** Box plots illustrate the average wPLI in the low alpha and low beta frequency bands, respectively, with the drumming epoch represented in the third column (indicated by the drum icon). Shamanic practitioners experienced statistically significant decreases in wPLI in the low alpha band and drumming compared to CC, as well as statistically significant increases in the low beta band. Significance is indicated by the key in the lower righthand corner of the figure.

Recent studies examining psychedelic-induced and shamanic states of consciousness have sought to characterize changes in neural signal diversity (Schartner et al., 2017; Huels et al. 2021), which represents the number of unique patterns within a signal. This approach is intuitive because, in line with the entropic brain hypothesis, it quantifies the uncertainty contained in time series data. These studies have characterized signal diversity through Lempel-Ziv complexity (LZc), which calculates the temporal complexity of a (finite) signal by calculating the number of distinct subsequences. A signal is regarded as complex if it is not possible to provide a brief representation of it: thus, regular signals are characterized by a small number of patterns (low LZc), whereas complex signals are characterized by larger number of patterns (high LZc): Following this reasoning, Mitchell (2009) identifies signal complexity with *richness of content*, which corresponds to the heightened sensory experiences of participants on psychedelics.

While LZc was initially invented as the basis of the zip compression algorithm (Lempel, 1976), it has since been adapted for signal analysis in neuroscience studies. For each epoch, the time series is first binarized using the median value (M) of the time series as a threshold, since the median is robust to outliers and invariant to signal amplitude (Huels et al. 2021):

$$s(n) = \{0 \text{ if } x(n) < M, 1 \text{ if } x(n) \geq M$$

where $x(n)$ is each data point of the original epoch. An example of this binarization can be seen in Figure 4.

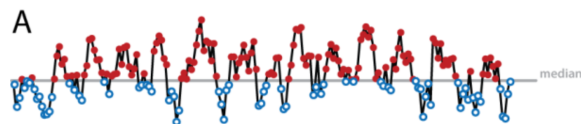


Figure 4. An example of LZc binarization, borrowed from Leemburg and Bassetti (2018). Red dots are represented by a 1, blue dots are represented by a 0.

After this, the binarized sequence is processed from the left, tallying each unique subsequence. For example, the input stream *01000101110010100101* would have nine unique subsequences: *0, 1, 00, 01, 011, 10, 010, 100, 101*. The final LZc score is computed as:

$$C(n) = c(n) * b(n)$$

where $c(n)$ is the number of unique subsequences, often normalized by the theoretical maximum number of subsequences $b(n) = n \log_2 n$.

In their study on psilocybin, ketamine, and LSD, Schartner and colleagues (2017) found that ketamine and LSD reliably increase LZc scores, while psilocybin did not (Figure 5), suggesting that different classes of psychedelics may have different impacts on the brain. The study on shamanic practitioners also did not find statistically significant increases in complexity—surprisingly, it found a statistically significant *decrease* in LZc in gamma bands (Huels et al., 2021). Drawing conclusions from these results is difficult, given the scarcity of LZc-based studies of altered states of consciousness. It is quite possible that inconsistencies in results are due to the computational method itself, since it operates on the complexity of a single signal, rather than evaluating global complexity across several nodes. Nevertheless, Schartner and colleagues' (2017) results demonstrate that some psychedelic substances do reliably increase Lempel-Ziv complexity.

Measure	PSIL (n=14)						KET (n=19)						LSD (n=15)					
	%	t	p	effect size %			%	t	p	effect size %			%	t	p	effect size %		
LZc	↑ 79	1.5	0.154	14	86	0	↑ 100	3.7	0.001	37	63	0	↑ 87	3.4	0.002	40	60	0
LZc _N	↑ 86	1.3	0.197	0	100	0	↑ 100	3.4	0.002	0	100	0	↑ 80	2.5	<i>0.018</i>	0	100	0
LZs	↑ 86	1.5	0.134	57	36	7	↑ 89	3.4	0.002	74	26	0	↑ 100	4.9	0.000	93	7	0
LZs _N	↑ 86	1.4	0.173	0	100	0	↑ 100	3.5	0.001	0	100	0	↑ 93	4.8	0.000	0	100	0

Part of Figure 5 on the following page.

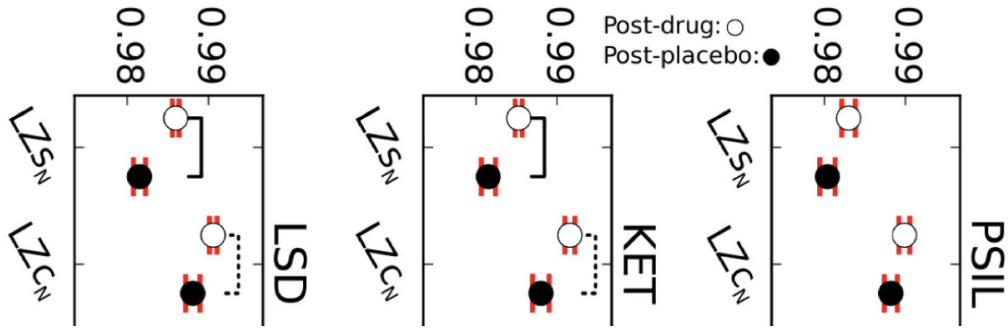


Figure 5. The above figures from Schartner et al. (2017) demonstrate the changes in increase in MEG signal diversity following ingestion of psilocybin, ketamine, and LSD, compared to placebo in the second chart. LZc and LZc_N are the unnormalized and normalized Lempel-Ziv complexities as outlined above, respectively. LZs_N is the normalized single-channel LZc, which captures temporal signal diversity only (LZc captures spatial signal diversity across MEG channels as well). In the second chart, the solid and dotted lines across conditions indicate $p < 0.001$ and $p < 0.05$, respectively. Results show that ingestion of LSD and ketamine resulted in increased signal diversity, while ingestion of psilocybin did not, suggesting that different classes of psychedelics may have different effects on the brain.

Criticality

Briefly explained in the introduction, criticality is a state occupying a narrow transition window between order and chaos, characterized by a maximum number of metastable or transiently-stable states, maximum sensitivity to perturbation (such as stimuli), and a propensity for cascade-like processes that propagate throughout the system, referred to as “avalanches” (Carhart-Harris et al., 2014). Many computational and experimental studies suggest that human brain functioning resides near a critical point during conscious wakefulness (Lee and Mashour,

2018) and reaches criticality in psychedelic-induced states and shamanic drumming (Carhart-Harris et al. 2014; Huels et al., 2021).

Intuitively, criticality and complexity are useful metrics for characterizing and distinguishing altered states of consciousness, such as those found in the psychedelic or shamanic brain. Maximum criticality and complexity, marked by maximum sensitivity to stimuli, indicates a more unconstrained and suggestible mode of cognition, less inhibited by high-level association networks and metacognitive (reality-checking) processes. Since these networks are responsible for functional integration, their inhibition gives more autonomy to more distributed activity, thus causing the variance of network synchrony to increase.

Criticality can be assessed using the pair correlation function (PCF), which computes the mean variance of network synchronization, reflecting network susceptibility to internal and external perturbations. Like LZc, the PCF indicates how much uncertainty there is in the network at any given time. (We will also see this with Shannon entropy in the graph theory section.)

$$PCF = N \{ \langle Re^2[z(t)] \rangle_t - \langle Re[z(t)] \rangle_t^2 \}$$

where $Re[z(t)]$ is the real part of $z(t)$:

$$z = r e^{i\psi} = \frac{1}{N} \sum_{j=1}^N e^{i\theta_j},$$

We can understand $z(t)$ as a vector of z values across timepoints, where z is the average phase angle across N nodes. The PCF function finds the variance of the average real component of this vector (across time) and multiplies it by the number of nodes N . It is important to note that PCF is maximal at a critical point and gradually decreases as a system moves toward a sub- or supercritical state (Kim and Lee, 2019). This is why criticality is an excellent metric to evaluate

altered states of consciousness: as entropy increases with disorder, criticality *decreases*. Thus, maximum criticality is a reliable characteristic of the psychedelic or shamanic brain.

As expected, Huels et al. (2021) found that during the shamanic healing exercise, the brains of shamanic practitioners experienced increased criticality (more precisely, increase in mean network synchrony variance) in the beta and gamma bands, which correspond to heightened alertness and awareness (Figure 6). It is important to note that the control group did not perform an intensive task during the drumming epoch, so we would possibly observe less high-frequency activity in their brains. However, this does not imply that the *variance in network synchrony* would decrease in those bands, so the results of the study are reliable. Furthermore, Carhart-Harris et al. (2014) demonstrated that the high-level association and integration networks (DMN, L-FP, R-FP, and Salience) had a statistically significant change in variance following psilocybin ingestion, compared to placebo (Figure 6). Although the authors did not mention using the PCF explicitly, they were measuring precisely the same phenomenon (mean variance of internal synchrony). Moreover, the study computed the probability distribution of the mean variance of internal synchrony in DMN signal following placebo and psilocybin ingestion, respectively, and found the distribution following psilocybin ingestion to be significantly wider.

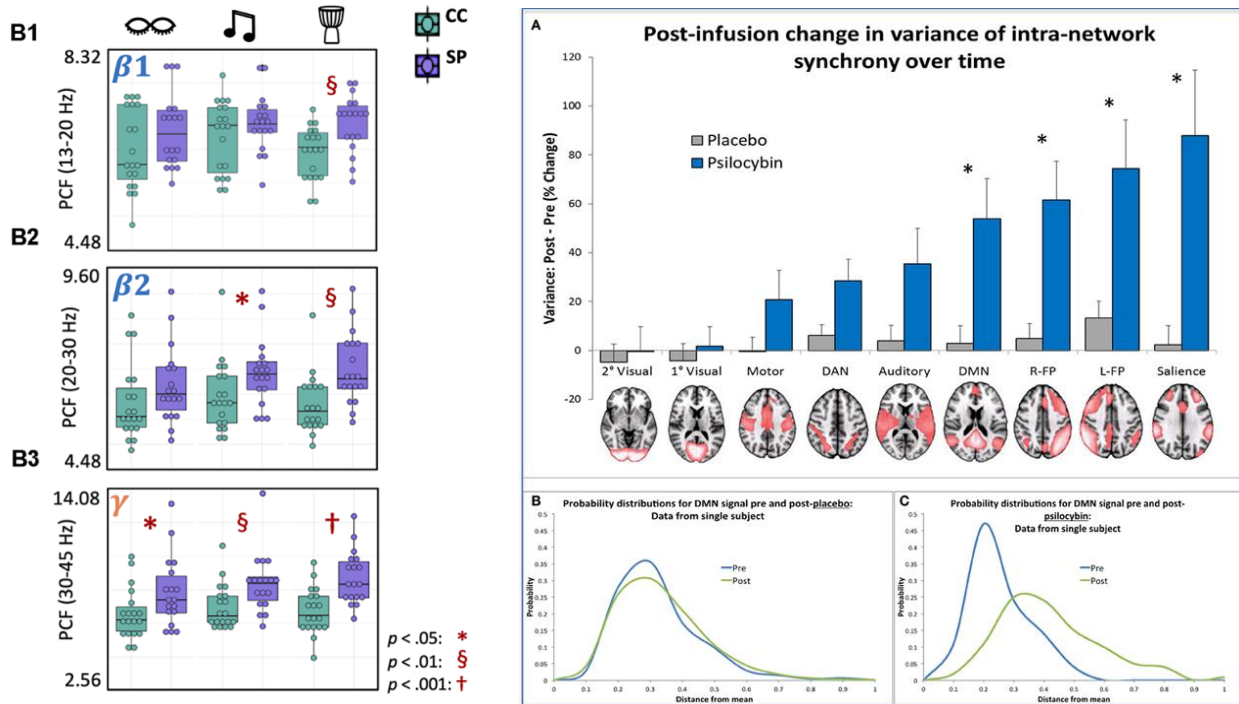


Figure 6. The collection of three graphs on the left from Huels et al. (2021) compare the PCF of shamanic practitioners (SP) and the control group (CC) during three activities (including drumming in the third column) and across three bands: **(B1)** low beta (13-20 Hz), **(B2)** high beta (20-30 Hz) and **(B3)** gamma (30-45 Hz). The study found that during drumming, the PCF was significantly greater among shamanic practitioners than the control group across all three bands. Significance is indicated by the key in the lower righthand corner of the figure. These bands correlate with the highest levels of alertness and awareness. // The collection of three graphs on the right from Carhart-Harris et al. (2014) demonstrate change in mean variance of internal synchrony of brain networks following placebo and psilocybin ingestion. Although the authors did not mention using the PCF, they were measuring precisely the same phenomenon (mean variance of internal synchrony). **(A)** Across nine brain regions, the high-level association and integration networks (DMN, L-FP, R-FP, and Salience) had a statistically significant change in mean variance ($p < 0.006$) following psilocybin ingestion, compared to placebo. **(B,C)** Taken

from a single subject, the authors computed the probability distribution of the mean variance of internal synchrony in DMN signal following placebo and psilocybin ingestion, respectively. Evidently, the distribution following psilocybin ingestion was significantly wider. The distributions were used to calculate Shannon entropy change, which was significantly greater in the same brain networks as in (A). We will explore Shannon entropy formally in the following section.

Network Theory Approach

Together, the three methods outlined in the previous section capture the increased connectivity, complexity, and criticality of that accompany elevated states of consciousness, thus corroborating the entropic brain hypothesis's claim that the psychedelic (or shamanic) brain is marked by increased uncertainty and variability in potential brain states. Because we are ultimately evaluating the degree and quality of connectivity, we can formalize the brain network by generating complex graphs to represent actual functional brain connectivity patterns. These networks can be generated by constructing a correlation matrix³ of time series from selected brain regions (fMRI data) or electrodes (EEG data). Alternatively, a functional connectivity matrix can be constructed using metrics such as the PLI. A thresholding function⁴ converts the absolute values of the correlation or connectivity matrix to an adjacency matrix⁵, which is used to generate complex graphs from which network characteristics and metrics can be calculated.

³ For example, Viol et al. (2017) used the Pearson correlation function.

⁴ In order to obtain better statistics, Viol et al. (2017) used a range of threshold values to ensure the network was fully-connected but relatively sparse. The lowest correlation threshold (corresponding to maximum mean degree) ensured that the networks had lower global efficiency and greater local efficiency than their randomized counterpart. The upper correlation threshold (minimum mean degree) ensured fully-connected graphs and guaranteed that the networks obey the sparsity condition $\langle k \rangle > 2 \ln N$, where N was the number of nodes. For more details, the reader is invited to read the original study.

⁵ For any two nodes i and j , element a_{ij} of an unweighted and undirected adjacency matrix is 1 if there exists an edge between the nodes (correlation passes threshold), and 0 if there does not exist an edge (correlation does not pass threshold).

While degree distribution and Shannon entropy may have significant impact on the following network properties—and thus give insight into the relative effects of psychedelics—they do not entirely define a network on their own. One can easily imagine an iso-entropic graph (with the same degree distribution) but with different connectivity. Thus, one can quantify the extent to which degree distribution and entropy influence network properties by comparing a given network to randomly generated iso-entropic networks⁶.

Mean characteristic path length

A geodesic or characteristic path (d_{ij}) is the number of edges in the shortest path between nodes i and j in a network. If there is no path between two nodes, the distance is defined as infinite. Given a network G with N nodes, the mean characteristic path length calculated as:

$$D(G) = \frac{1}{N(N-1)} \sum_{i \neq j} d_{i,j}.$$

Following the findings and hypotheses outlined in this paper, we would expect $D(G)$ to decrease (as connectivity increases) in altered states of consciousness, since more connections imply shorter distances between nodes. However, Viol and colleagues (2017) found that globally, mean path length actually *increases* following ayahuasca ingestion (Figure 7). While surprising at first, these findings actually do make sense, since global integration networks are *suppressed* by psychedelics, promoting more local connectivity. Thus, following the inhibition of the rich

⁶ Viol and colleagues (2017) approached this task using the Maslov algorithm, in which two non-overlapping pairs of linked nodes (e.g. (i, j) and (m, n) , arbitrarily) are repeatedly selected, unlinked, and then cross-linked into (i, m) and (j, n) , thus conserving node degree and, by extension, degree distribution. As the study showed, clustering, mean characteristic path length, and efficiency are sometimes conserved following randomization. Thus, by comparing the observed graph in study participants to iso-entropic networks, one can distinguish effects that are susceptible to specific topological arrangements, as opposed to those due to changes in degree distribution. For more details, the reader is invited to read the original study.

club of densely-connected integration hubs, mean path length increases globally. When compared to iso-entropic networks, mean path length was not conserved (Viol et al., 2017), indicating that ayahuasca inhibits high-level integration networks in a unique way.

Clustering coefficient

This metric quantifies the density of triads of linked nodes—in other words, the fraction of the neighbors of a node that are themselves neighbors. It is defined as:

$$C(G) = \frac{1}{N} \sum_{i \neq j \neq h} \frac{2}{k_i(k_i - 1)} a_{i,j} a_{j,h} a_{h,i},$$

where k_i is the degree of node i and a is the adjacency matrix element. The fraction inside the sum represents the maximum number of edges between neighbors of each node, given that node's degree (e.g. the maximum number of nodes between neighbors of a node with degree 4 is indeed $2/(4 * 3) = 12$). Notice that any element of the sum is non-zero only if all three adjacency matrix elements are themselves non-zero, i.e. when all three nodes are connected to each other.

Following our understanding that psychedelics promote connectivity, we would expect an increase in clustering in altered states of consciousness, since more connections imply shorter distances between nodes. Indeed, Viol and colleagues (2017) found that clustering increases following ayahuasca ingestion, compared to placebo (Figure 7). When compared to iso-entropic networks, however, clustering was largely conserved, suggesting that the modularization of connectivity itself is a key feature of the psychedelic brain, rather than a unique local topography.

Efficiency

Efficiency quantifies the influence of network topology on the flux of information throughout the network, and is defined as the reciprocal of the harmonic mean of geodesic distances. Global efficiency is defined as

$$E_g(G) = \frac{1}{N(N-1)} \sum_{i \neq j \in G} \frac{1}{d_{i,j}},$$

and local efficiency as

$$E_l(G) = \frac{1}{N} \sum_{i \in G} \left(\frac{1}{n_i(n_i-1)} \sum_{j \neq h \in g_i} \frac{1}{d_{h,j}} \right),$$

where g_i are the subnetworks formed by neighbors of node i and n_i is the number of nodes in the particular subnetwork.

Drawing on the logic outlined previously, we would expect *global* efficiency to decrease in altered states, following the decrease in fluency of high-level association and reality-checking prediction networks. On the other hand, we would expect *local* efficiency to increase in altered states, given the increase in modular connectivity, which allows information to flow more easily through the subnetworks. Indeed, these hypotheses are corroborated by the findings of Viol and colleagues (2017), outlined in Figure 7. When compared to iso-entropic networks, global efficiency was not conserved, indicating that ayahuasca inhibits high-level integration networks in a specific way. On the other hand, local efficiency was conserved, suggesting that the modularization and increase of connectivity itself is a key feature of the psychedelic brain, rather than a unique local topography.

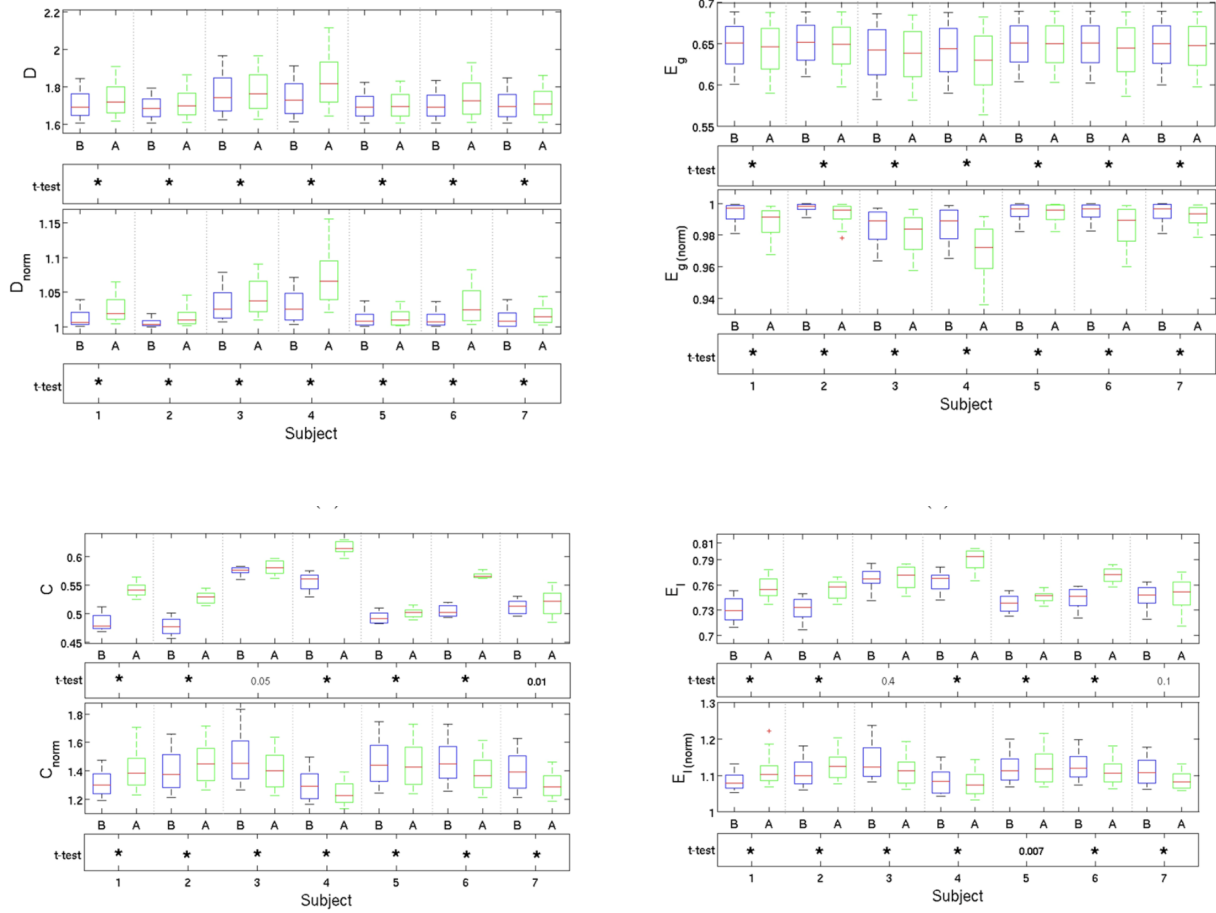


Figure 7. The four charts above, from Viol et al. (2017), starting clockwise from the top left, demonstrate the change in mean geodesic distance, global efficiency, local efficiency, and clustering, all unnormalized and normalized, in brain networks of 7 participants before and after ingestion of the psychedelic ayahuasca. All t-tests marked with * had a statistically significant p -value of $p < 0.005$, with the rest indicating the p -value at which they were statistically significant. Results show that following ingestion, mean geodesic distance and global efficiency decreased, while local efficiency and clustering increased.

Degree distribution

This metric evaluates the degree distributions of nodes in the network, often represented as a normalized histogram, where degree k_j of node j is the number of edges the node shares with other nodes (see Figure 8 for examples from Viol et al., 2017). One would expect the variance of the degree distribution to increase in the psychedelic-induced brain, on account of the increase in entropy and connectivity (Figure 8).

Shannon entropy

In addition to the aforementioned standard network properties, studies such as Viol et al. (2017) used Shannon entropy to quantify uncertainty or disorder in the network. In particular, Shannon entropy is calculated as a function of the distribution of node degrees, as mentioned above. If $P(k)$ is the normalized probability distribution for node degree k (i.e. $\sum_k P(k) = 1$), Shannon entropy is defined as:

$$S[P] = -\sum_k P(k) \log P(k).$$

Unsurprisingly, in line with the wider degree distribution histogram following ayahuasca ingestion, Viol et al. (2017) found the brain networks of these participants to exhibit higher Shannon entropy than the control group (Figure 8). This metric formalizes what many of the other outlined computations methods have stood as correlates of—namely, the number of possible states the network can assume (the amount of uncertainty in the system).

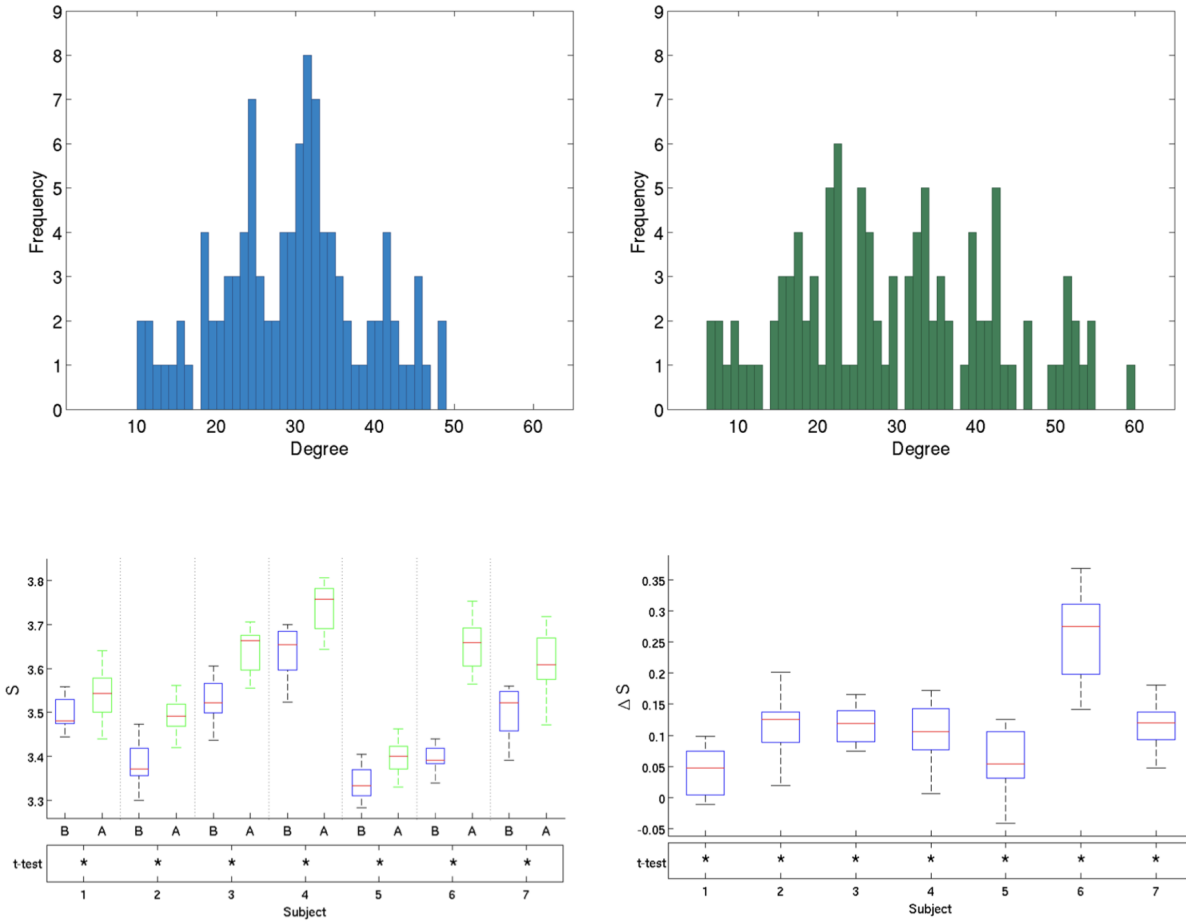


Figure 8. The four charts above, from Viol et al. (2017), demonstrate the change in degree distribution and Shannon entropy in brain networks of 7 participants before and after ingestion of the psychedelic ayahuasca. The blue and green histograms plot the average degree distribution before and after ingestion, respectively. The two box-and-whiskers plots show the Shannon entropy before and after ingestion (S) and the change in entropy (ΔS) for each participant, respectively. Together, the data demonstrate a statistically significant ($p < 0.005$) increase in entropy following ingestion for all participants.

Conclusion

All of the computational methods and empirical findings outlined in this paper are tightly coupled with the entropic brain hypothesis, since each method addresses an aspect of entropy, connectivity, or complexity that accompanies altered states of consciousness. Lempel-Ziv complexity characterizes the uniqueness of neural signals, which corresponds to the number of transiently-stable states the brain can occupy. The pair correlation function and Shannon entropy are both measures of variance: the former of network synchrony and the latter of degree distribution. Crucially, Shannon entropy (and other network characteristics) can only be calculated based on functional connectivity metrics (such as the PLI), which define the edges in the graph. Thus, it is only through a comprehensive, synthetic understanding of all of these computational methods that we can appreciate the mechanistic and experiential features of altered states of consciousness, and how they relate to other states.

References

- Carhart-Harris, R., Leech, R., Hellyer, P., Shanahan, M., Feilding, A., & Tagliazucchi, E. et al. (2014). The entropic brain: a theory of conscious states informed by neuroimaging research with psychedelic drugs. *Frontiers In Human Neuroscience*, 8. <https://doi.org/10.3389/fnhum.2014.00020>
- Cohen, M. (2015). Effects of time lag and frequency matching on phase-based connectivity. *Journal Of Neuroscience Methods*, 250, 137-146. <https://doi.org/10.1016/j.jneumeth.2014.09.005>
- Eickhoff, S., & Müller, V. (2015). Functional Connectivity. *Brain Mapping*, 187-201. <https://doi.org/10.1016/b978-0-12-397025-1.00212-8>
- Fludd, R. (1619). *Utriusque cosmi maioris scilicet et minoris ... historia* [Image]. Retrieved 11 April 2022, from <https://en.wikipedia.org/wiki/Consciousness#/media/File:RobertFuddBewusstsein17Jh.png>.

- Friston, K. (1994). Functional and effective connectivity in neuroimaging: A synthesis. *Human Brain Mapping*, 2(1-2), 56-78. <https://doi.org/10.1002/hbm.460020107>
- Friston, K. (2010). The free-energy principle: a unified brain theory?. *Nature Reviews Neuroscience*, 11(2), 127-138. <https://doi.org/10.1038/nrn2787>
- Huels, E., Kim, H., Lee, U., Bel-Bahar, T., Colmenero, A., & Nelson, A. et al. (2021). Neural Correlates of the Shamanic State of Consciousness. *Frontiers In Human Neuroscience*, 15. <https://doi.org/10.3389/fnhum.2021.610466>
- Kim, H., & Lee, U. (2019). Criticality as a Determinant of Integrated Information Φ in Human Brain Networks. *Entropy*, 21(10), 981. <https://doi.org/10.3390/e21100981>
- Lee, U., & Mashour, G. (2018). Role of Network Science in the Study of Anesthetic State Transitions. *Anesthesiology*, 129(5), 1029-1044. <https://doi.org/10.1097/aln.0000000000002228>
- Leemburg, S., & Bassetti, C. (2018). Lempel-Ziv complexity of the EEG predicts long-term functional recovery after stroke in rats. <https://doi.org/10.1101/248039>
- Lempel, A., & Ziv, J. (1976). On the Complexity of Finite Sequences. *IEEE Transactions On Information Theory*, 22(1), 75-81. doi: 10.1109/tit.1976.1055501
- Mitchell, M. (2011). *Complexity*. Oxford University Press.
- Petri, G., Expert, P., Turkheimer, F., Carhart-Harris, R., Nutt, D., Hellyer, P., & Vaccarino, F. (2014). Homological scaffolds of brain functional networks. *Journal Of The Royal Society Interface*, 11(101), 20140873. <https://doi.org/10.1098/rsif.2014.0873>
- Schartner, M., Carhart-Harris, R., Barrett, A., Seth, A., & Muthukumaraswamy, S. (2017). Increased spontaneous MEG signal diversity for psychoactive doses of ketamine, LSD and psilocybin. *Scientific Reports*, 7(1). <https://doi.org/10.1038/srep46421>
- Stam, C., Nolte, G., & Daffertshofer, A. (2007). Phase lag index: Assessment of functional connectivity from multi channel EEG and MEG with diminished bias from common sources. *Human Brain Mapping*, 28(11), 1178-1193. <https://doi.org/10.1002/hbm.20346>
- Subramaniam, N. (2019). *EEG Connectivity Using Phase Lag Index - Sapien Labs | Neuroscience | Human Brain Diversity Project*. Sapien Labs | Neuroscience | Human Brain Diversity Project. Retrieved 11 April 2022, from <https://sapienlabs.org/lab-talk/eeg-connectivity-using-phase-lag-index/>.

Thiagarajan, T., Lebedev, M., Nicolelis, M., & Plenz, D. (2010). Coherence Potentials: Loss-Less, All-or-None Network Events in the Cortex. *Plos Biology*, 8(1), e1000278. <https://doi.org/10.1371/journal.pbio.1000278>

Vinck, M., Oostenveld, R., van Wingerden, M., Battaglia, F., & Pennartz, C. (2011). An improved index of phase-synchronization for electrophysiological data in the presence of volume-conduction, noise and sample-size bias. *Neuroimage*, 55(4), 1548-1565. <https://doi.org/10.1016/j.neuroimage.2011.01.055>

Viol, A., Palhano-Fontes, F., Onias, H., de Araujo, D., & Viswanathan, G. (2017). Shannon entropy of brain functional complex networks under the influence of the psychedelic Ayahuasca. *Scientific Reports*, 7(1). <https://doi.org/10.1038/s41598-017-06854-0>